Am J Transl Res 2021;13(12):13452-13461
www.ajtr.org /ISSN:1943-8141/AJTR0135238

Original Article

miR-34a overexpression protects against hippocampal neuron damage caused by ketamine-induced anesthesia in immature rats through the Notch-1/NF-κB signaling pathway

Xueyan Li[1*], Genshan Ma[2*], Chun Zhang[1], Mo Chen[1], Xiaochen Huang[1], Chengyong Gu[1]

[1]Suzhou Hospital of Nanjing Medical University, Suzhou Municipal Hospital (North District), Suzhou 215000, Jiangsu, China; [2]Tumor Hospital Affiliated to Nantong University, Nantong Tumor Hospital, Nantong 226001, Jiangsu, China. [*]Co-first authors.

Received May 14, 2021; Accepted October 20, 2021; Epub December 15, 2021; Published December 30, 2021

Abstract: Objective: To investigate the protective effect of miR-34a overexpression on hippocampal neuron damage caused by ketamine-induced anesthesia in immature rats and the underlying mechanism. Methods: A total of 48 male SD rats were divided into control group (CG, n=12), ketamine group (KG, n=12), negative control group (NCG, n=12), and intervention group (IG, n=12) by using the random number table method. Neurological function, cognitive function, pathological changes of brain tissues, inflammatory cytokines, as well as mRNA expression levels of Notch-1, NICD, RBP-JK, and Hes-1 in brain tissues were detected in the four groups. Results: The scores of auricular, paw withdrawal, corneal reflex, and escape reflexes of IG were higher than those of KG and NCG (P<0.05). At day 3 after intervention, the escape latency, time of staying in the quadrants of original platform, and times of crossing the quadrants of original platform of IG were lower than those of KG and NCG (P<0.05). HE staining results revealed that the morphology and structure of a few neurons and glial cells in IG were changed, and the intercellular space was increased. The brain tissues of NCG demonstrated marked neuron damage with unclear structure; these changes were less significant for KG. The levels of TNF-α, IL-1β, and IL-6 of IG were lower than those of KG and CG (P<0.05). Conclusions: miR-34a overexpression exhibited a potent protective effect on hippocampal neuron damage caused by ketamine-induced anesthesia in immature rats.

Keywords: miR-34a overexpression, Notch-1/NF-κB signaling pathway, ketamine-induced anesthesia, hippocampal neuron, protective effect

Introduction

Ketamine is an anesthetic with low blood/air partition coefficient, stable hemodynamics, and rapid recovery [1, 2]. It is widely used in a variety of minor operations, clinical diagnostic procedures, and general anesthesia induction. Although ketamine is considered a weak anesthetic, researchers have reported that exposure to ketamine in the developing brain may cause hippocampal neuron damage and lead to severe neuronal apoptosis and neurodegenerative changes [3, 4]. The impact is often manifested through impaired development for learning and memorizing, cognitive function, and behaviors in the long run. Clinical studies have revealed that ketamine can cause neurotoxicity in immature brain tissues or brain tissues with systemic infection [5]. Ketamine can induce long-term dysplasia of brain function, affect the metabolic pathway of brain tissues and cause neurotoxicity of the brain.

MicroRNAs (miRNAs) are endogenous non-coding RNAs that contain 22 nucleotides; they are widely present in cells and play multiple regulatory roles in cellular metabolic processes [6]. miR-34a is a type of miRNA that regulates protein expression through complete or partial complementary association with a target mRNA [7, 8]. Notch-1/NF-κB signaling pathway is known for its highly protective and critical roles

in evolution. It is one of the few signal transduction systems that can repeatedly regulate cell proliferation, apoptosis, and differentiation [9]. Meanwhile, Notch-1/NF-κB pathway is one of the key signaling pathways that regulate neuronal apoptosis. Based on this, the purpose of this study was to investigate the protective effect of miR-34a overexpression on hippocampal neuron damage caused by ketamine-induced anesthesia in immature rats through the regulation of Notch-1/NF-κB signaling pathway.

Materials and methods

Animal experiment

A total of 48 clean-grade specific pathogen-free (SPF) male SD rats were divided into four groups by using the random number table method, including control group (CG, n=12, intraperitoneally injected with 75 mg/kg of normal saline), ketamine group (KG, n=12, intraperitoneally injected with 75 mg/kg ketamine), negative control group (NCG, n=12, intraperitoneally injected with 75 mg/kg ketamine + intrathecally injected with 5 μL/d negative control lentivirus at a titer of 5×10^8 TU/mL), and intervention group (IG, n=12, intraperitoneally injected with 75 mg/kg ketamine + intrathecally injected with 5 μL miR-34a lentivirus) (animal quarantine certificate number: SCXX-2005-0001). All rats were raised in a laboratory-grade animal room (temperature, 22±2°C; humidity, 50±10%). Animals were fed normally in the light and had unlimited access to food and water. All operations in this study met the ethical requirements of animal experiments, and were reviewed and approved by the Ethics Committee of Suzhou Hospital of Nanjing Medical University (No. KL901071).

Instruments and equipment

The following instruments and equipment were used: rat cages (Animal Experimental Center of Xi'an Jiaotong University, China); phenobarbital sodium for injection (New Asiatic Pharmaceutical, China); RFQ-PCR detection kit (Beijing Guangsuo Labao Science and Technology Co., Ltd., China); paraformaldehyde (Sinopharm Chemical Reagent Co. Ltd., China); neutral balsam (Zsbio Commerce Store, China); BCM-1000A bio-clean bench (Bio-Equip, China); table-type high-speed and low-temperature centrifuge machine (Herolab, Germany); fluorescent quantitative polymerase chain reaction (PCR) (Genetimes Technology Inc., China); enzyme-linked immunosorbent assay (ELISA) detector (Bio Tek, USA); vibratome (LEICA, Germany); miR-34a lentivirus/negative control lentivirus (Shanghai Genechem Co. Ltd., China); SYBR Green Master Mixture (TAKARA, Japan); ELISA kit (R&D Systems, USA); and NF-kB rabbit polyclonal antibody/β-actin rabbit monoclonal antibody (Santa Cruz, USA).

Establishment and treatment of animal models

Establishment of animal models: According to previously reported methods, rats were weighed accurately prior to the establishment of the immature rat models with hippocampal neuron damage caused by ketamine-induced anesthesia [10]. To this end, KG rats were intraperitoneally injected with 75 mg/kg ketamine to induce hippocampal neuron damage. Rat models were considered successful if they exhibited symptoms such as reduced activities, slow response, tachypnea, reduced food and water intake or hypouresis [11].

Intervention methods: KG rats were intraperitoneally injected with 75 mg/kg ketamine for 3 consecutive days. NCG rats were intraperitoneally injected with 75 mg/kg ketamine and intrathecally injected with 5 μL/d negative control lentivirus according to the liposome transfection instructions using Lipofectamine 3000 (Fisher Scientific, USA) (at a titer of 5×10^8 TU/mL) for 3 consecutive days. IG rats were intraperitoneally injected with 75 mg/kg ketamine and intrathecally injected with 5 μL miR-34a lentivirus (at a titer of 5×10^8 TU/mL) for 3 consecutive days. CG rats were intraperitoneally injected with the same amount of normal saline for three consecutive days.

Neurological function scores and cognitive function test

Neurological function scores: All rats were treated for three consecutive days. Neurological function was measured in terms of auricle, paw withdrawal, corneal and pupillary light, and escape reflexes. Each item was evaluated using a three-level scoring method (0, 1 and 2). The lower score represented the poorer neurological function [12].

Table 1. Primer sequence

Type	Primer	Length
β-actin	F: 5' CAGGATGCAGCAGGTGGAAGC 3' R: 5' TGCTCCAGGCTGTAGTCTGTGG 3'	132
Notch-1	F: 5' AGGTTCCTCTCCTAGCAGATCATTCTC 3' R: 5' GAGCGGCAACTTCTGAGGTCTTAC 3'	99
NICD	F: 5' GCTGAGTCCTCTTGCTGTGCTC 3' R: 5' GTACCTGGAGGCTTGGCATGAC 3'	158
RBP-JK	F: 5'-TTGGAAGGATGGCATACAC-3' R: 5'-CAATGAAGTTGACTGGACTC-3'	84
Hes-1	F: 5'-GGAGCGAGATCCCTCCAAAAT-3' R: 5'-GGCTGTTGTCATACTTCTCATGG-3'	79
NF-KB	Forward: 5'-TGGTGGGCCGCAGAACATGTGC-3' Reverse: 5'-GCGAGCACAGAATTAATACGAC-3'	25
iNOS	Forward: 5'-TTGGAAGGATGGCATACAC-3' Reverse: 5'-CAATGAAGTTGACTGGACTC-3'	58
IL-lβ	Forward: 5'-GGAGCGAGATCCCTCCAAAAT-3' Reverse: 5'-GGCTGTTGTCATACTTCTCATGG-3'	41
miR-34a	Forward: 5'-ATCCCTTACCAAGCTTAGGA-3' Reverse: 5'-CCGTATTACTGTAGGTTCTC-3'	20

Cognitive function test: Cognitive function was assessed at day 3 after intervention using the water maze and open field tests. The specific methods are detailed as follows.

(1) Water maze test. The Morris water maze was an oval maze 120 cm in diameter and 60 cm in height, with the water temperature controlled at 22-26°C. The pool consisted of four quadrants 5 cm below the surface of water. Escape latency was measured using a navigation test. Spatial probe test was used to record the time of staying in the quadrants of original platform and the times of crossing the quadrants from the original platform within 60 s.

(2) Open field test. A square and transparent top container was used as an open field test case (with 25 square lattices at the bottom and 9 in the center regarded as the central zone). Rats were placed in the central zone for free moving up to 15 min to record the time of staying in the central zone [13].

Pathological changes of brain tissues

After intervention, deep anesthesia was induced. After the induction anesthesia took effect, the rats were routinely disinfected and prepared for surgical draping. Brain tissues were collected, dehydrated, paraffin-embedded, and subjected to HE staining. The pathological changes of brain tissues were observed under an inverted microscope [14, 15].

Levels of inflammatory cytokines

Blood (5 mL) was collected from the caudal vein after the completion of intervention. After centrifugation, the levels of TNF-α, IL-1β, IL-6 and IL-10 in brain tissues were measured using ELISA.

mRNA levels in brain tissues

Trizol (500 μL) was added to the brain tissue samples prepared in the previous step. After intensive mixing, the samples were transferred into centrifuge tubes (1.0 mL) for a 5-minute vibration and left to stand. Serum samples from the two groups were added with 200 μL chloroform for a 5-second vibration and left to stand for 5 min, then centrifuged for 15 min at 1,216 rpm. After the supernatant was discarded, 1 mL pre-cooled ethanol (concentration: 75.0%) was added and dried for 7 min. DNA concentration of samples was estimated by measuring the optical density at 260 nm using a UV spectrophotometer.

Detection methods: RFQ-PCR was used to measure the mRNA expression of Notch-1, NICD, RBP-JK, and Hes-1, as well as the inflammatory cytokines, such as NF-KB, p-NF-KB, iNOS, and IL-lβ in the brain tissues. PCR parameters were set as follows: 30°C for 10 min; 42°C for 30 min; 99°C for 5 min; and 5°C for 5 min, 35 cycles in succession, and an elongation step at 72°C for 10 min. The PCR products were separated using 1.5% agar gel electrophoresis. β-actin was used as the internal control. Primers used are listed in **Table 1** [16, 17].

Protein expression of brain tissues

Western blot was used to measure the protein expression of Notch-1, NICD, RBP-JK, and Hes-1, as well as the inflammatory cytokines such as NF-κB, p-NF-κB, iNOS, and IL-lβ in brain tissues. Specific steps included extraction of proteins, SDS-PAGE of proteins, transfer of proteins, incubation with primary and secondary antibodies, and image development. A small amount of luminous liquid was added to the

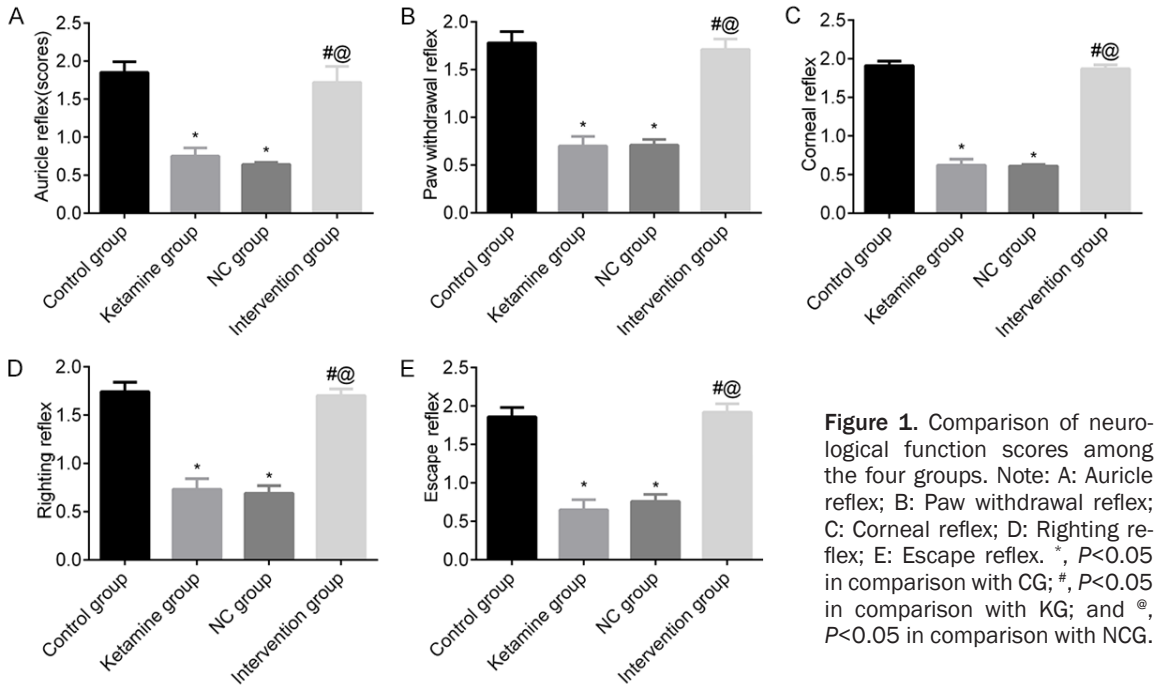

Figure 1. Comparison of neurological function scores among the four groups. Note: A: Auricle reflex; B: Paw withdrawal reflex; C: Corneal reflex; D: Righting reflex; E: Escape reflex. *, $P<0.05$ in comparison with CG; #, $P<0.05$ in comparison with KG; and @, $P<0.05$ in comparison with NCG.

final PVDF membrane to develop the image under proper exposure conditions [18].

Statistical analysis

SPSS 18.0 software was used for statistical analysis. The data represented by n (%) were analyzed by χ^2 test. The data represented by $\bar{x}$ ±sd were analyzed by *t*-test. $P<0.05$ implied a statistically significant difference.

Results

Neurological function scores

The scores of auricle, paw withdrawal, corneal, righting and escape reflexes in KG and NCG were significantly lower than those in CG ($P<0.05$). While those in IG were significantly higher than those in KG and NCG ($P<0.05$). These findings indicated that the up-regulation of miR-34a expression could significantly improve the neurological function deficit caused by ketamine-induced anesthesia in immature rats, as shown in **Figure 1**.

Cognitive function

The Morris water maze test at day 3 after intervention showed that the escape latency of KG and NCG rats was notably longer than that of CG rats, and the indicators of KG and NCG were significantly lower than those of CG in terms of the time of staying at quadrants of original platform, times of crossing quadrants of original platform, and open field test on the 1st, 2nd, and 3rd days ($P<0.05$). The escape latency of IG was markedly shorter than that of KG and NCG, and the indicators of IG were significantly higher than those of KG and NCG in terms of the time of staying at quadrants of original platform, times of crossing quadrants of original platform, and open field test on the 1st, 2nd, and 3rd days ($P<0.05$). These findings implied that the up-regulation of miR-34a expression could significantly improve the cognitive impairment caused by ketamine-induced anesthesia in immature rats, as shown in **Figure 2**.

Pathological changes of brain tissues

The neurons and glial cells in CG showed a clear morphology and structure; an increased intercellular space was observed in few cells in IG. Significant neuronal damage was observed in the brain tissues of NCG, and a large number of glial cells were lost and the structure disordered. KG also showed neuronal damage, loss of glial cells, structural disorder and other pathological changes, which were slightly less than those of NCG. Details are shown in **Figure 3**.

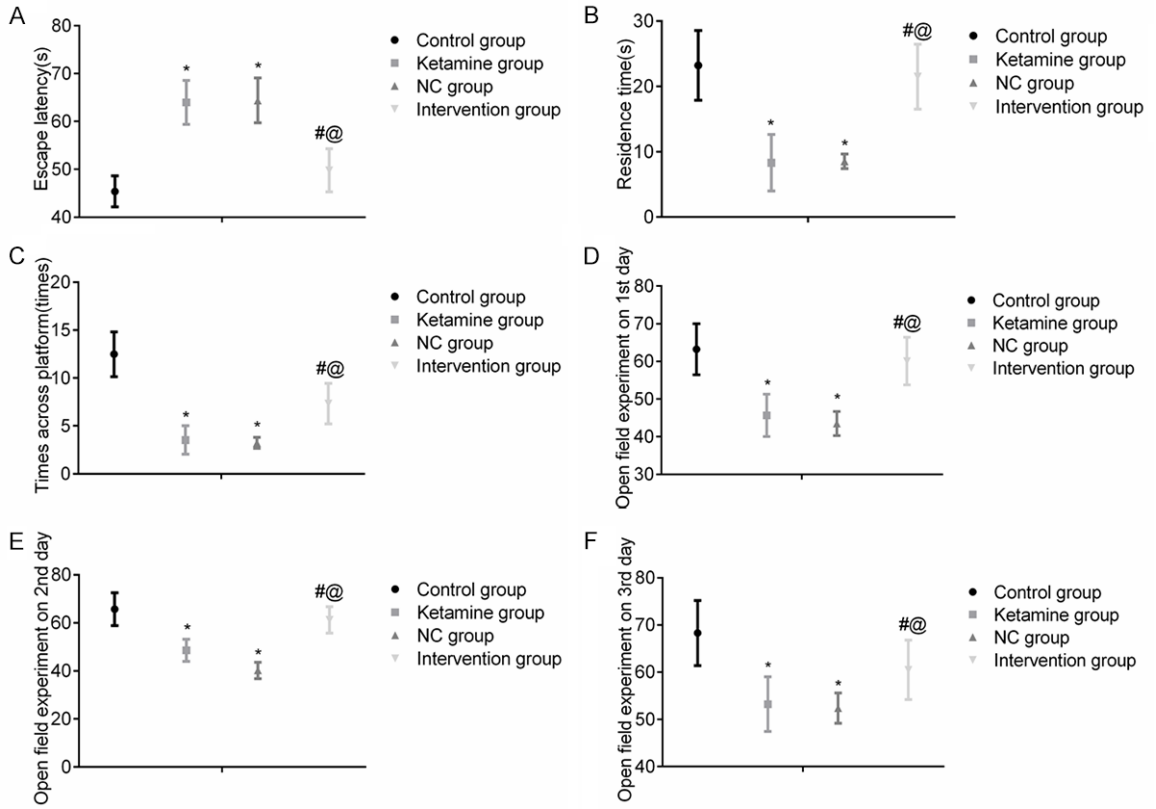

Figure 2. Comparison of cognitive function among four groups. Note: A: Escape latency; B: Residence time; C: Time across platform; D: Open field test on the 1st day; E: Open field test on the 2nd day; F: Open field test on the 3rd day. *, $P<0.05$ in comparison with CG; #, $P<0.05$ in comparison with KG; and @, $P<0.05$ in comparison with NCG.

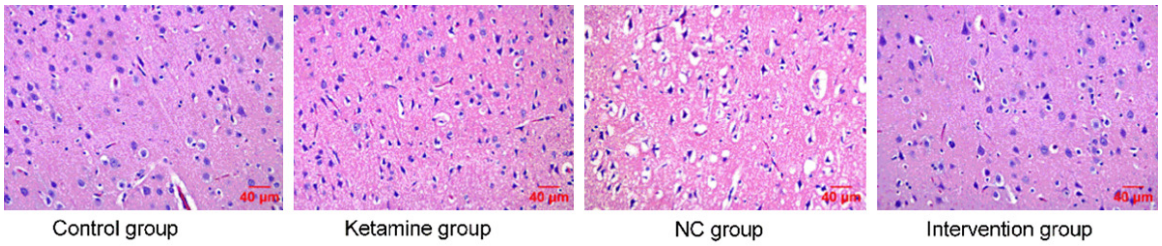

Figure 3. HE staining results of four groups (×200).

Levels of inflammatory cytokines in brain tissues

The levels of TNF-α, IL-1β, and IL-6 in the brain tissues of KG and NCG were higher than those of CG, while IL-10 level was lower than that of CG, and the difference was statistically significant (all $P<0.05$). The levels of TNF-α, IL-1β, and IL-6 in IG were lower and IL-10 level was higher than those in KG and NCG after intervention ($P<0.05$). This implied that the up-regulation of miR-34a expression could notably alleviate the inflammatory injury in the brain tissues of immature rats with neuronal damage caused by ketamine-induced anesthesia, as shown in **Figure 4**.

mRNA expression level of Notch-1, NICD, RBP-JK and Hes-1

The Notch-1 level of KG and NCG was lower than that of CG ($P<0.05$), while the levels of NICD, RBP-JK, and Hes-1 were higher than those of CG (all $P<0.05$). The Notch-1 level of IG was higher than that of KG and NCG after intervention ($P<0.05$). The levels of NICD, RBP-JK,

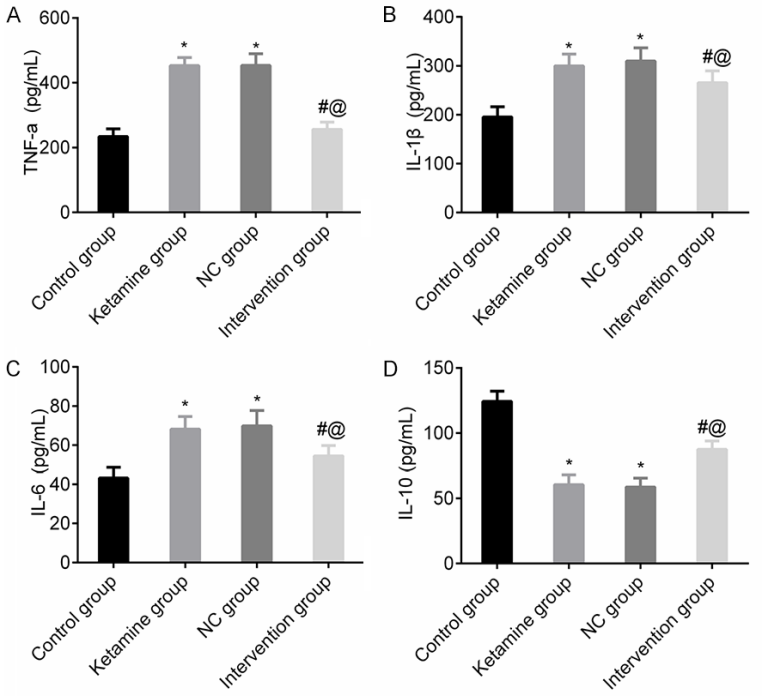

Figure 4. Comparison of inflammatory cytokine levels among four groups. Note: A: TNF-α; B: IL-1β; C: IL-6; D: IL-10. *, *P*<0.05 in comparison with CG; #, *P*<0.05 in comparison with KG; and @, *P*<0.05 in comparison with NCG.

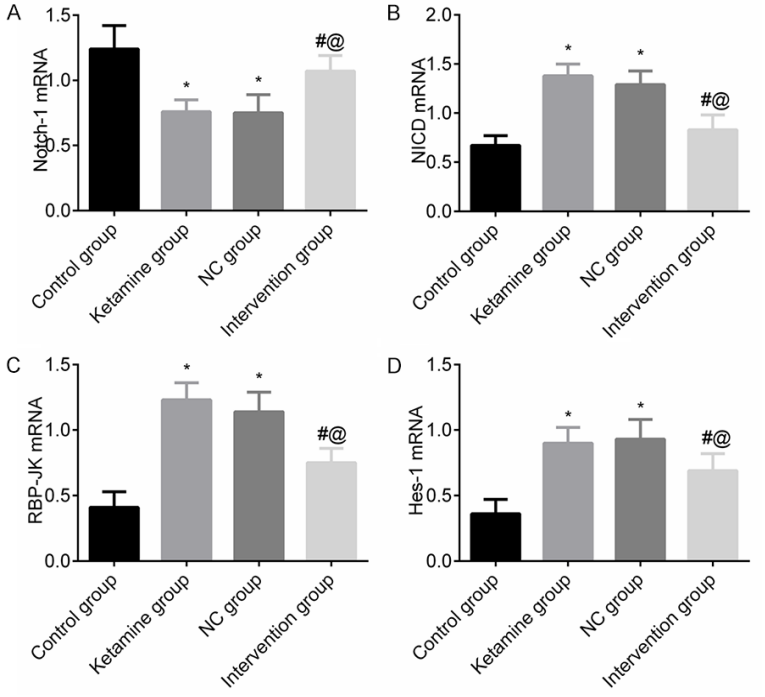

Figure 5. Comparison of mRNA expression levels of Notch-1, NICD, RBP-JK and Hes-1 in brain tissues among four groups. Note: A: Notch-1 mRNA; B: NICD mRNA; C: RBP-JK mRNA; D: Hes-1 mRNA. *, *P*<0.05 in comparison with CG; #, *P*<0.05 in comparison with KG; and @, *P*<0.05 in comparison with NCG.

and Hes-1 of IG were lower than those of KG and NCG (*P*<0.05). Details are shown in **Figure 5**.

mRNA levels of NF-KB, iNOS, and IL-lβ in brain tissues

The mRNA levels of NF-κB, iNOS, and IL-lβ of KG and NCG were significantly higher than those of CG (*P*<0.05). The mRNA levels of NF-κB, iNOS, and IL-lβ of IG were much lower than those of KG and NCG after intervention (*P*< 0.05). Details are shown in **Figure 6**.

Proteins related to the Notch-1/NF-κB signaling pathway in brain tissues

Western blot results are shown in **Figures 7**, **8**. Consistent with the expression pattern of mRNA, the protein expression levels of Notch-1 of KG and NCG were lower than those of CG (*P*<0.05), while the protein expression levels of NICD, RBP-JK, and Hes-1 as well as the inflammatory cytokines such as p-NF-κB, iNOS, and IL-lβ of KG and NCG were higher than those of CG (all *P*<0.05). After intervention, the protein expression of Notch-1 of IG was higher than that of KG and NCG (*P*<0.05), and the protein expression levels of NICD, RBP-JK, and Hes-1 as well as the inflammatory cytokines such as p-NF-κB, iNOS, and IL-lβ of IG were lower than those of KG and NCG (*P*<0.05).

Discussion

Ketamine is an anesthetic commonly used in clinical practice. It has high lipophilicity, which is 5-10 times greater than that of thiopental sodi-

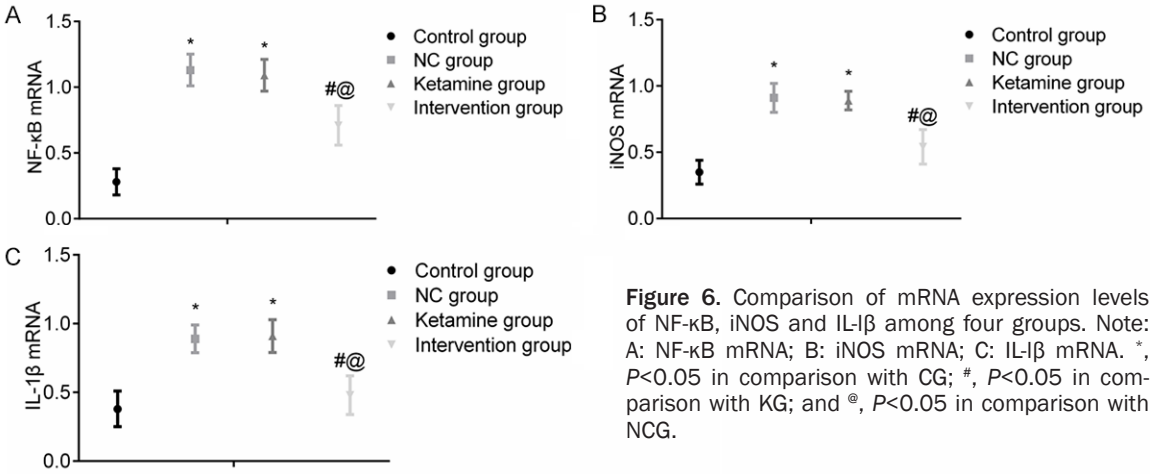

Figure 6. Comparison of mRNA expression levels of NF-κB, iNOS and IL-Iβ among four groups. Note: A: NF-κB mRNA; B: iNOS mRNA; C: IL-Iβ mRNA. *, $P<0.05$ in comparison with CG; #, $P<0.05$ in comparison with KG; and @, $P<0.05$ in comparison with NCG.

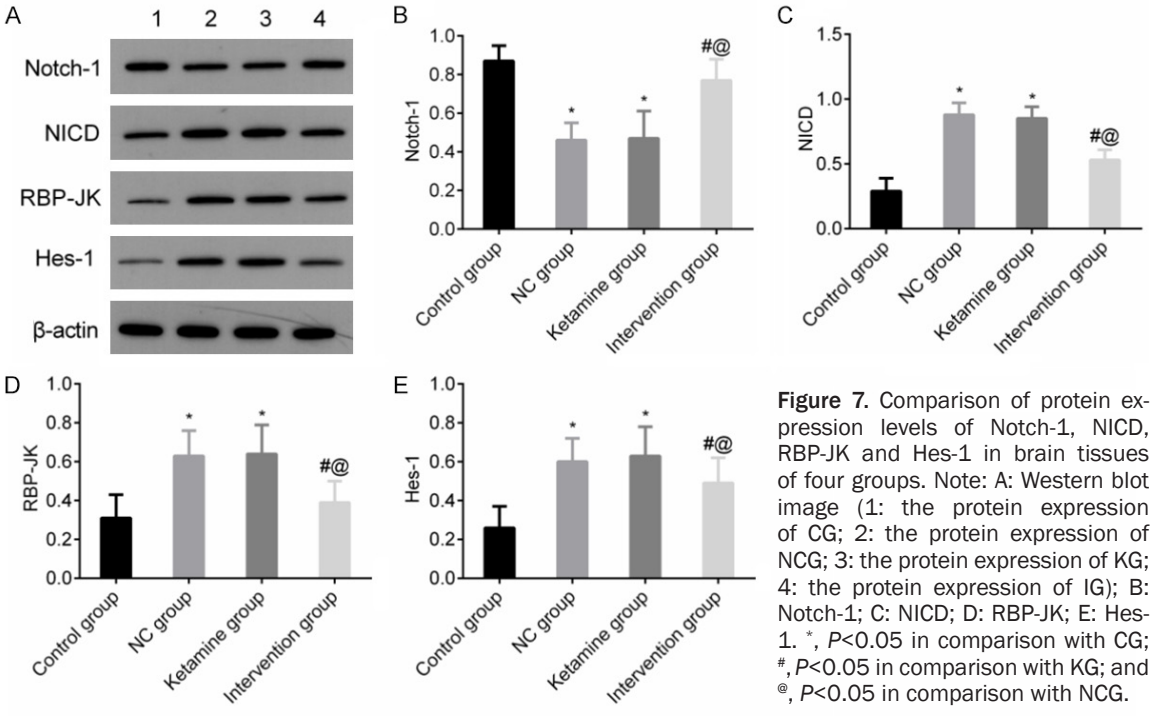

Figure 7. Comparison of protein expression levels of Notch-1, NICD, RBP-JK and Hes-1 in brain tissues of four groups. Note: A: Western blot image (1: the protein expression of CG; 2: the protein expression of NCG; 3: the protein expression of KG; 4: the protein expression of IG); B: Notch-1; C: NICD; D: RBP-JK; E: Hes-1. *, $P<0.05$ in comparison with CG; #, $P<0.05$ in comparison with KG; and @, $P<0.05$ in comparison with NCG.

um. After injection, ketamine can rapidly penetrate the central nervous system, causing the loss of consciousness. The drug effect lasts 10-15 min. Clinical studies have shown that patients may experience frequent nystagmus after a light level of anesthesia induced by an appropriate dose of intravenous injection of ketamine. However, some patients may suffer from intensive and obvious stimuli due to increased muscle tension and blocked thalamic and cortical pathways [19, 20]. HE staining results in this study showed obvious neuronal damage in the brain tissues of NCG and KG, observed as unclear morphology and structure in neurons and glial cells. In IG, the morphology and structure of a few neurons and glial cells were ameliorated and exhibited an increased intercellular space. This indicated the successful establishment of immature rat models with hippocampal neuron damage caused by ketamine-induced anesthesia in this study, thus laying the foundation for future experiments.

At present, the pathogenesis of hippocampal neuron damage caused by ketamine-induced anesthesia in immature rats is still unclear. It

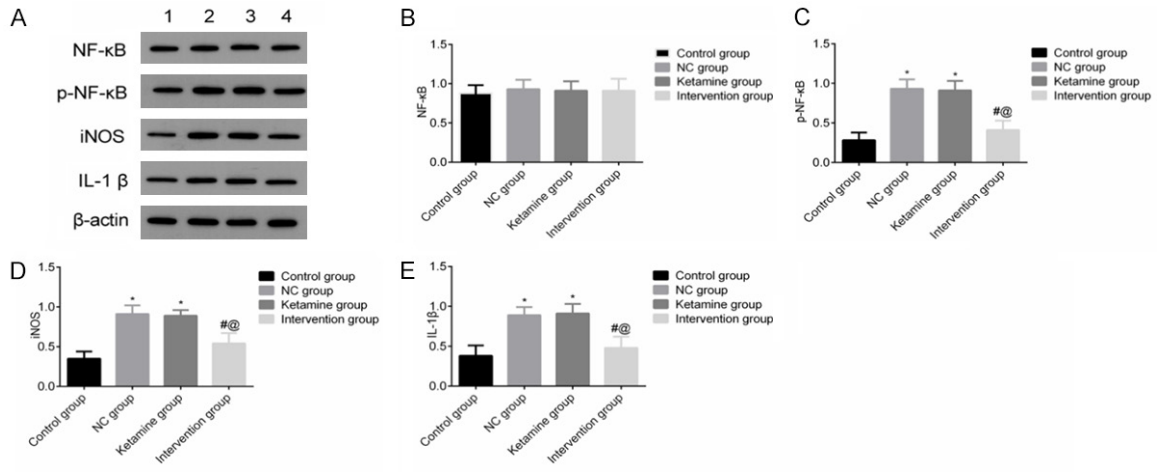

Figure 8. Comparison of protein expression levels of NF-κB, p-NF-κB, iNOS and IL-Iβ among the four groups. Note: A: Western blot image (1: the protein expression of CG; 2: the protein expression of NCG; 3: the protein expression of KG; 4: the protein expression of IG); B: NF-κB; C: p-NF-κB; D: iNOS; E: IL-Iβ. *, $P<0.05$ in comparison with CG; #, $P<0.05$ in comparison with KG; and @, $P<0.05$ in comparison with NCG.

may be related to the inflammatory response. A visceral or systemic inflammatory response is detected in the brain through the vagus nerve and the circumventricular organs based on changes in endorphin and autonomic nerve nuclei. After the activity signal is transmitted to the brain, large amounts of inflammatory and anti-inflammatory cytokines are released to activate endothelial cells, thereby damaging the blood-brain barrier and causing the central nervous system symptoms [21]. In this study, the levels of TNF-α, IL-1β, and IL-6 of IG were lower than those of KG and NCG, and the level of IL-10 of IG was higher than that of KG and CG after intervention. This indicated that miR-34a overexpression could reduce the level of inflammatory cytokines in the brain tissues of immature rats. The Notch-1/NF-κB signaling pathway is an important metabolic pathway in the human body. Notch-1 is a key transcription factor involved in inflammatory cytokines in the nucleus and is present in cells of the nervous system. It participates in the amplification of the inflammatory response and increases the gene expression of various factors. Besides, Notch-1 may be involved in the occurrence of an inflammatory response by extending the gene expression of cytokines. At the same time, the Notch signaling pathway is also a key link in the development of multiple organs and systems, including Notch receptor, Notch ligand, and DNA-binding protein CSL. When Notch1 is cleaved under signal stimulation and releases its activated form of N1-ICD fragment, it transfers to the nucleus and binds with the nuclear factor RBP-JK to form an energy complex and initiate downstream genes of the Notch pathway, such as Hes1 [22]. A study has indicated that Notch receptor can activate the NF-κB signaling pathway, regulate the systemic inflammatory response, reduce ischemic brain injury, and thus up-regulate the NF-κB signaling pathway [23]. In this study, the Notch-1 level of IG was higher than that of KG and NCG, and the levels of NICD, RBP-JK, Hes-1 mRNA, NF-KB, p-NF-KB, iNOS, and IL-Iβ mRNA of IG were lower than those of KG and NCG after intervention. The results of Western blot were consistent with those of gene detection. This implied that miR-34a overexpression had a potent protective effect on hippocampal neuron damage caused by ketamine-induced anesthesia in immature rats, indicating the down-regulation of the Notch-1/NF-κB signaling pathway.

miRNA is a small non-coding RNA that plays an important biological role in the human body. It inhibits the expression of related genes through 3'UTR in the target gene mRNA. Another study has demonstrated that miR-34a is one of the miRNAs involved in novel mechanisms of post-transcriptional regulation of gene expression [24]; moreover, it plays an important role in immune response, development, and inflammatory responses [25]. A previous report has indicated that miR-34a plays a specific role in

the Notch-1/NF-κB signaling pathway, directly regulating inflammatory and immune responses and the proliferation and growth of tumor stem cells [26]. In this study, the escape latency of IG was shorter than that of KG and NCG. The indicators of IG were higher than those of KG and NCG in terms of the time of staying at the quadrants of original platform, times of crossing quadrants of the original platform, and open field test on the 1st, 2nd, and 3rd days. These results implied that miR-34a overexpression had a potent protective effect on hippocampal neuron damage caused by ketamine-induced anesthesia in immature rats, with little influence on cognitive function. Therefore, the results provide new insights into clinical treatment modalities.

In conclusion, miR-34a overexpression has a potent protective effect on hippocampal neuron damage caused by ketamine-induced anesthesia in immature rats. It can reduce the level of inflammatory cytokines in the brain tissues, indicating its effect on the Notch-1/NF-κB signaling pathway.

Disclosure of conflict of interest

None.

Address correspondence to: Chengyong Gu, Suzhou Hospital of Nanjing Medical University, Suzhou Municipal Hospital (North District), No. 242 Guangjinan Road, Jiangsu District, Suzhou 215000, Jiangsu, China. Tel: +86-0512-62363036; Fax: +86-0512-62363036; E-mail: chengyonggu100@163.com

References

[1] Gibori H, Eliyahu S, Krivitsky A, Ben-Shushan D, Epshtein Y, Tiram G, Blau R, Ofek P, Lee JS, Ruppin E, Landsman L, Barshack I, Golan T, Merquiol E, Blum G and Satchi-Fainaro R. Amphiphilic nanocarrier-induced modulation of PLK1 and miR-34a leads to improved therapeutic response in pancreatic cancer. Nat Commun 2018; 9: 16.

[2] Shi K, Sun H, Zhang H, Xie D and Yu B. miR-34a-5p aggravates hypoxia-induced apoptosis by targeting ZEB1 in cardiomyocytes. Biol Chem 2019; 400: 227-236.

[3] Guennewig B, Roos M, Dogar AM, Gebert LF, Zagalak JA, Vongrad V, Metzner KJ and Hall J. Synthetic pre-microRNAs reveal dual-strand activity of miR-34a on TNF-α. RNA 2014; 20: 61-75.

[4] Soliman B, Salem A, Ghazy M, Abu-Shahba N and El Hefnawi M. Bioinformatics functional analysis of let-7a, miR-34a, and miR-199a/b reveals novel insights into immune system pathways and cancer hallmarks for hepatocellular carcinoma. Tumour Biol 2018; 40: 1010428318773675.

[5] Rao BD, Shrivastava S, Pal S and Chattopadhyay A. Effect of local anesthetics on the organization and dynamics of hippocampal membranes: a fluorescence approach. J Phys Chem B 2019; 123: 639-647.

[6] Jiang S, Wu Y, Fang DF and Chen Y. Hypothermic preconditioning but not ketamine reduces oxygen and glucose deprivation induced neuronal injury correlated with downregulation of COX-2 expression in mouse hippocampal slices. J Pharmacol Sci 2018; 137: 30-37.

[7] Jiang Y, Zhou Y, Ma H, Cao X, Li Z, Chen F and Wang H. Autophagy dysfunction and mTOR hyperactivation is involved in surgery: induced behavioral deficits in aged C57BL/6J Mice. Neurochem Res 2020; 45: 331-344.

[8] Zou S, Wei ZZ, Yue Y, Zheng H, Jiang MQ and Wu A. Desflurane and surgery exposure during pregnancy decrease synaptic integrity and induce functional deficits in juvenile offspring mice. Neurochem Res 2020; 45: 418-427.

[9] Mijailovic N, Selakovic D, Joksimovic J, Mihailovic V, Katanic J, Jakovljevic V, Nikolic T, Bolevich S, Zivkovic V, Pantic M and Rosic G. The anxiolytic effects of atorvastatin and simvastatin on dietary-induced increase in homocysteine levels in rats. Mol Cell Biochem 2019; 452: 199-217.

[10] Ji MH, Xia DG, Zhu LY, Zhu X, Zhou XY, Xia JY and Yang JJ. Short- and long-term protective effects of melatonin in a mouse model of sepsis-associated encephalopathy. Inflammation 2018; 41: 515-529.

[11] Park EJ, Appiah MG, Myint PK, Gaowa A, Kawamoto E and Shimaoka M. Exosomes in sepsis and inflammatory tissue injury. Curr Pharm Des 2019; 25: 4486-4495.

[12] Shimada T, Topchiy E, Leung AKK, Kong HJ, Genga KR, Boyd JH, Russell JA, Oda S, Nakada TA, Hirasawa H and Walley KR. Very low density lipoprotein receptor sequesters lipopolysaccharide into adipose tissue during sepsis. Crit Care Med 2020; 48: 41-48.

[13] Choi WJ, Li Y and Wang RK. Monitoring acute stroke progression: multi-parametric OCT imaging of cortical perfusion, flow, and tissue scattering in a mouse model of permanent focal ischemia. IEEE Trans Med Imaging 2019; 38: 1427-1437.

[14] Farahany NA, Greely HT, Hyman S, Koch C, Grady C, Pașca SP, Sestan N, Arlotta P, Bernat JL, Ting J, Lunshof JE, Iyer EPR, Hyun I,

Capestany BH, Church GM, Huang H and Song H. The ethics of experimenting with human brain tissue. Nature 2018; 556: 429-432.

[15] Das S, Mukherjee U, Pal S, Maitra S and Sahoo P. Selective sensing of Al(3+) ions by nitrophenyl induced coordination: imaging in zebrafish brain tissue. Org Biomol Chem 2019; 17: 5230-5233.

[16] Trautz F, Dreßler J, Stassart R, Müller W and Ondruschka B. Proposals for best-quality immunohistochemical staining of paraffin-embedded brain tissue slides in forensics. Int J Legal Med 2018; 132: 1103-1109.

[17] Molina-Romero M, Gómez PA, Sperl JI, Czisch M, Sämann PG, Jones DK, Menzel MI and Menze BH. A diffusion model-free framework with echo time dependence for free-water elimination and brain tissue microstructure characterization. Magn Reson Med 2018; 80: 2155-2172.

[18] Bikis C, Rodgers G, Deyhle H, Thalmann P, Hipp A, Beckmann F, Weitkamp T, Theocharis S, Rau C, Schulz G and Müller B. Sensitivity comparison of absorption and grating-based phase tomography of paraffin-embedded human brain tissue. Appl Phys Lett 2019; 114: 083702.

[19] Lee S, Kim M, Oh JH, Lee JH, Shin N, Park T, Lee JH, Kim MC and Lee YJ. Optimized liquid chromatography-tandem mass spectrometry for Otaplimastat quantification in rat plasma and brain tissue. J Chromatogr Sci 2019; 57: 258-264.

[20] Huang X, Dai Z, Cai L, Sun K, Cho J, Albertine KH, Malik AB, Schraufnagel DE and Zhao YY. Endothelial p110γPI3K mediates endothelial regeneration and vascular repair after inflammatory vascular injury. Circulation 2016; 133: 1093-1103.

[21] Danahy DB, Anthony SM, Jensen IJ, Hartwig SM, Shan Q, Xue HH, Harty JT, Griffith TS and Badovinac VP. Polymicrobial sepsis impairs bystander recruitment of effector cells to infected skin despite optimal sensing and alarming function of skin resident memory CD8 T cells. PLoS Pathog 2017; 13: e1006569.

[22] Tzou WS, Lo YT, Pai TW, Hu CH and Li CH. Stochastic simulation of notch signaling reveals novel factors that mediate the differentiation of neural stem cells. J Comput Biol 2014; 21: 548-567.

[23] Ye G, Ye L, Zhou J, Shi L, Yang L and Dong Z. Challenges in diagnosing community-acquired carbapenem-susceptible Acinetobacter baumannii enterogenic sepsis: a case report. Medicine (Baltimore) 2019; 98: e16248.

[24] Lan P, Wang SJ, Shi QC, Fu Y, Xu QY, Chen T, Yu YX, Pan KH, Lin L, Zhou JC and Yu YS. Comparison of the predictive value of scoring systems on the prognosis of cirrhotic patients with suspected infection. Medicine (Baltimore) 2018; 97: e11421.

[25] Bernotiene E, Palmer G, Talabot-Ayer D, Szalay-Quinodoz I, Aubert ML and Gabay C. Delayed resolution of acute inflammation during zymosan-induced arthritis in leptin-deficient mice. Arthritis Res Ther 2004; 6: R256-263.

[26] Lee N, Cao B, Ke C, Lu H, Hu Y, Tam CHT, Ma RCW, Guan D, Zhu Z, Li H, Lin M, Wong RYK, Yung IMH, Hung TN, Kwok K, Horby P, Hui DSC, Chan MCW and Chan PKS. IFITM3, TLR3, and CD55 gene SNPs and cumulative genetic risks for severe outcomes in chinese patients with H7N9/H1N1pdm09 influenza. J Infect Dis 2017; 216: 97-104.